IMPACT OF COLLISION MODELS ON PARTICLE TRANSPORT IN OPEN CHANNEL FLOW

Bernhard Vowinckel
Institute of Fluid Mechanics
TU Dresden
D-01062 Dresden, Germany
Bernhard.Vowinckel@tu-dresden.de

Tobias Kempe
Institute of Fluid Mechanics
TU Dresden
D-01062 Dresden, Germany
Tobias.Kempe@tu-dresden.de

Jochen Fröhlich
Institute of Fluid Mechanics
TU Dresden
D-01062 Dresden, Germany
Jochen.Froehlich@tu-dresden.de

ABSTRACT

Simulation of sediment transport in turbulent channel flows is of vital interest in various applications such as environmental or biomedical flows. While the interaction of the fluid and the particle can be tackled numerically using a phase-resolved immersed boundary method (IBM), the particle-particle interaction has to be modeled using an appropriate collision model. This paper presents a sensitivity analysis for the particle-laden flow in a turbulent channel with respect to the type of collision model employed.

MODELLING OF PARTICLE COLLISION

The simulations carried out in this study were performed with the IBM proposed in Uhlmann (2005) modified as described in Kempe *et al.* (2009). The forces acting on a particle during collision can be decomposed into normal and tangential forces. In the present study a repulsive potential model (RPM) proposed by Glowinski *et al.* (2001) is used as well as the newly developed adaptive collision time model (ACTM) (Kempe et al, 2009; Kempe & Fröhlich, 2010b) In the latter case, the forces acting in the normal direction $\mathbf{n}_{pq}$ between particle p colliding with particle q are modelled according to

$$\mathbf{F}_{n,pq}^{col} = (k_n \zeta_n^{3/2} + d_n g_{n,pq})\,\mathbf{n}_{pq} \tag{1}$$

with $\zeta_{n,pq}$ being the gap between two colliding particles, g_n the relative normal particle velocity, k_n the material stiffness and d_n a damping coefficient for normal collision, both appropriately calibrated for each individual collision to yield the correct restitution coefficient while using a time step adequate for the flow physics ($CFL \approx 1$). The collision process hence is stretched in time.

The tangential forces are accounted for as follows (Haff & Werner, 1986). For rolling motion they are determined by

$$\mathbf{F}_{t,pq}^{col} = d_t\, g_t^{cp}\, \mathbf{t}_{pq} \tag{2}$$

with d_t the tangential coefficient of friction and g_t^{cp} the relative tangential velocity at the contact point. If $\mathbf{F}_{t,pq}^{col} \geq \mu_f |F_n|$ with μ_f being an empirical coefficient of friction, the rolling motion turns into a sliding motion described by

$$\mathbf{F}_{t,pq}^{col} = \mu_f |F_n|\, \mathbf{t}_{pq} \tag{3}$$

Since the collision process is stretched in time, this also affects the tangential component. It can be shown, however, that the momentum exchange between collion partners is unaffected (Kempe & Fröhlich, 2011).

When two particles approach each other, fluid is squeezed out of the gap. Immediately before and after the surfaces touch, this gap becomes smaller than the step size h of the grid. Hence, a lubrication model (Cox & Brenner, 1967)

$$\mathbf{F}_{n,pq}^{lub} = -\frac{6\pi\mu_f g_{n,pq}}{\zeta_{n,pq}} \left(\frac{R_p R_q}{R_p + R_q} \right) \tag{4}$$

is used for surface distances $\zeta_{n,pq}$ smaller than $2h$ to account for this effect with R being the particle radius (Kempe & Fröhlich, 2010) .

Using the ACTM, the total force acting on a particle reads

$$\mathbf{F}_p = \sum_{p,q \neq p}^{N_p} \mathbf{F}_{n,pq}^{col} + \mathbf{F}_{t,pq}^{col} + \mathbf{F}_{n,pq}^{lub} \tag{5}$$

Instead of modelling all these forces the original RPM only

accounts for normal forces setting

$$\mathbf{F}_p = \varepsilon m_p g \left(\max \left\{ 0, -\frac{\zeta_{n,pq} - S}{S} \right\} \right)^2 \mathbf{n}_{pq} \qquad (6)$$

where ε is a model constant, m_p the particle mass, S the range of the repulsive force, and g the gravitational acceleration. Since lubrication forces are not accounted for, the repulsive range has to be defined as $S = 2h$ to avoid unresolved fluid in the gap between two particles. The model constant ε was calibrated to guarantee a minimal resolution of five timesteps per collision.

These two approaches give rise to four different options with increasing complexity to model particle collision: RPM without tangential forces (Glowinski), RPM with tangential forces (Glowinski + HW), ACTM without tangential forces (ACTM), ACTM with tangential forces (ACTM + HW).

COMPUTATIONAL SETUP FOR SENSITIVITY ANALYSIS

Two different setups of open channel flow with periodic conditions in the streamwise and spanwise direction and a free slip condition on the upper boundary are considered to study the effects of the above collision models on sediment transport (Tab. 1), designed according to the experiments of Cameron *et al.* (2006). Since the goal of this study was a sensitivity analysis of the different collsion models, a rather small box of $L_x/H = 6$ and $L_z/H = 3$ with H the depth was used. This is about the minimum to guarantee decorrelated velocity fields for the proper employment of the periodic boundary conditions.

The goal of Setup I was to study the effects on particle trajectories of a single particle placed on top of a hexagonally packed sediment package (Fig. 1). The exposed particle was mobilised by the well-developed turbulent channel flow and statistics of the particle trajectory, the velocities of the particle and the forces exerted on the particle by the fluid were recorded over a large period in time.

Table 1. Key parameters of the different setups used to analyse the collision models.

Setup	Re_b	ρ_p/ρ_f	L_x/D	L_z/D
I	4449	1.25 ... 2.25	72	36
II	3010	1.2	52	27
Setup	H/D	Re_τ	D^+	D/Δ_x
I	12	263	22	14
II	9	219	25	20

For the simulations of Setup II, 500 particles were placed on top of a hexagonally packed sediment bed in order to study the effects of collision modelling on sediment transport, (Fig. 2). The Reynolds number of both setups was chosen to be rather high in order to simulate a wide range of possible motion of the particle. For the sake of computational costs, particles were reolved with $\Delta_x^+ = 1.57$ (in wall units) for Setup I and $\Delta_x^+ = 1.25$ for Setup II. The Froude number defined as

$$Fr = \frac{(\rho_p - \rho_f)\, g H}{\rho_f u_b^2} \qquad (7)$$

with ρ_p the particle density, ρ_f the fluid densitiy, and u_b the bulk velocity, estimates the ratio of gravitational forces to particle inertia.

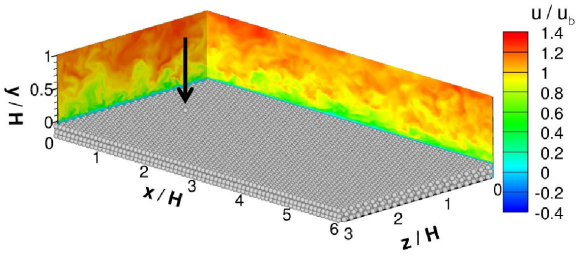

Figure 1. Setup I according to Tab. 1 used to study the effect of collision modelling on single particle trajectories. Contour plots represent the instantaneous streamwise velocity component. The arrow points at the exposed particle.

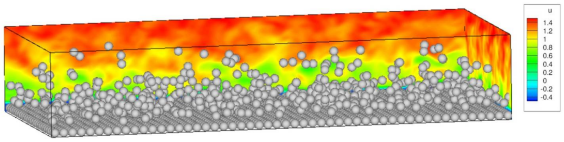

Figure 2. Setup II according to Tab. 1 used to study the effect of collision modelling on sediment transport. Countours as in Fig 1.

RESULTS FOR SINGLE PARTICLE MOBILE

States of motion

Particle trajectories differ systematically depending on the state of motion of the particle between two collisions (Fig. 3). This behavior was also found in experiments performed by Lajeunesse *et al.* (2010), who distinguished between three different kinematic states: resting, creeping, and jumping. Therefore, the average velocity between two points of collision $\langle \mathbf{u}_p \rangle_{ball}$ can be taken as a critical parameter to distinguish between a resting and a creeping state (the index ball refers to "ballistic"). Since a large increase in the jumping length was observed when the velocity exceeded $\langle \mathbf{u}_p \rangle_{ball,crit} = 0.01\, u_b$, this value was taken as a threshold between resting and creeping.

The creeping state is characterized by a rolling or sliding motion of the particle and a strong interaction with the sediment bed, i.e. a large number of collisions per lenght of path. The jumping state in turn only shows a weak interaction with the sediment bed. Thus the threshold to distinguish

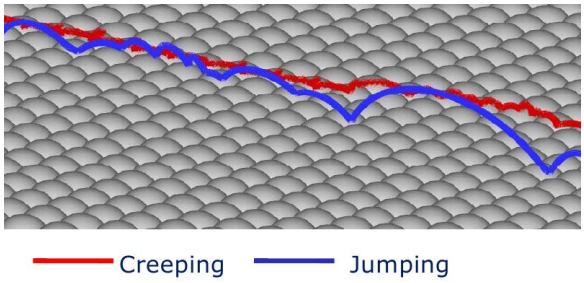

Figure 3. Particle tracejecories with different states of motion.

between creeping and jumping is defined here in terms of the distance between two collisions $\zeta_{jump,crit}$ and depends on the local geometry of the sediment bed. This value is chosen here as the distance between two local minima of elevation in the sediment bed. The present hexagonal packing yields $\zeta_{jump,crit} = D\sqrt{3}/3 = 0.58D$. This is in agreement with Lajeunesse *et al.* (2010), who used a value of $0.9D$ for cubical packing.

Since all three states occur for a given trajectory of a particle, the simulated trajectory was subdivided into the three kinematic states. Afterwards, selected physical parameters (e.g. linear and angular velocity components) were conditionally averaged over individual particle trajectories and subsequently over all trajectories to determine these quantities in the kinematic states.

Results for jumping state

To evaluate the impact of the four collision models in the jumping state, Probability Density Functions (PDFs) of ω_3 (the angular componentin spanwise direction) and H_{ball} (the jumping height of a particle) are shown in Fig. 4 and 5.

In the jumping regime the PDF of ω_3 becomes Gaussian, i.e. the interaction with the local geometry of the sediment bed decreases (Fig. 4). Thus the PDF of ω_3 is influenced by the viscous stresses acting on the particle only. With increasing height above the sediment bed, the viscous stresses acting on the particle decrease resulting in a lower angular velocity. If a tangential model is employed, the angular velocities increase. This can be observed for both, the ACTM and the Glowinski model, being more pronounced for the latter. Fig. 5 shows the PDF of the jumping height of the particle in the jumping regime. The trajectories simulated with the ACTM have slightly smaller jumping heights. The arrangement of the peaks of the PDF shown in Fig. 5 is in agreement with the oberservation from Fig. 4: more frequent jumps of low heigth leads to an increase of angular velocity.

Results for creeping state

The impact of the four collision models on the creeping state becomes obvious by plotting the PDFs of u_p (the linear, streamwise velocity component) and ω_3 which are shown in Fig. 6 and 7. As can be seen from Fig. 6 the mean linear velocity is lower with the ACTM compared to the RPM. This is an effect caused by the repulsive range $S = 2h$ used in the Glowinski model. The mobile particle therefore is hovering

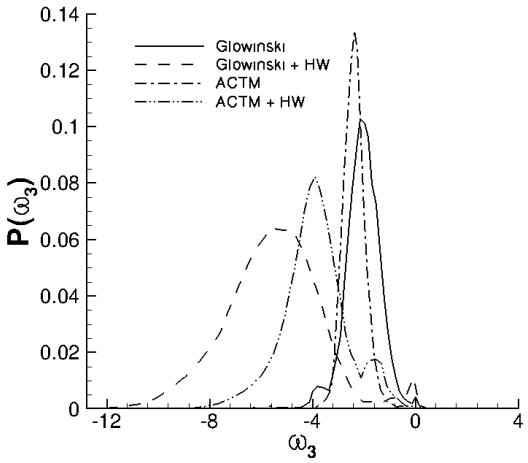

Figure 4. Probability density function of the angular velocity (rotation around spanwise axis) of the particle in jumping state.

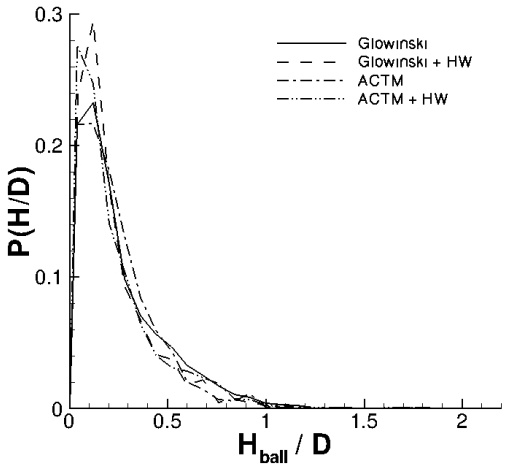

Figure 5. Probability density function of the jumping height of the particle in jumping state.

at a distance of about $2h$ above the sediment bed and is penetrating deeper into the turbulent boundary layer than with the ACTM. This leads to higher pressure forces and visous forces on the creeping particle if the RPM is used.

A somewhat similar effect can be seen in Fig. 7. Again, if the RPM is used with or without a tangential model, the particle has higher rotational velocities so that, in total, the RPM yields higher kinetic energy, angular and linear. Moreover, the use of the tangential model leads to an increase of rotational velocities. This increase is due to the fact that the spinning behavior caused by the viscous stresses can actually be translated into a rolling motion if a tangential model is used.

It can be found in experiments (e.g. Lajeunesse et al., 2010) that if the particle exhibits a strong interaction with the sediment bed, i.e. the jumping length approaches zero, the particle travels along the sediment bed with a rolling motion. Thus,

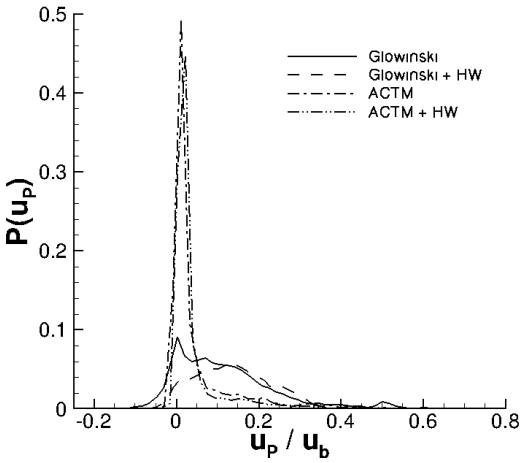

Figure 6. Probability density function of the linear, streamwise velocity component of the particle in creeping state.

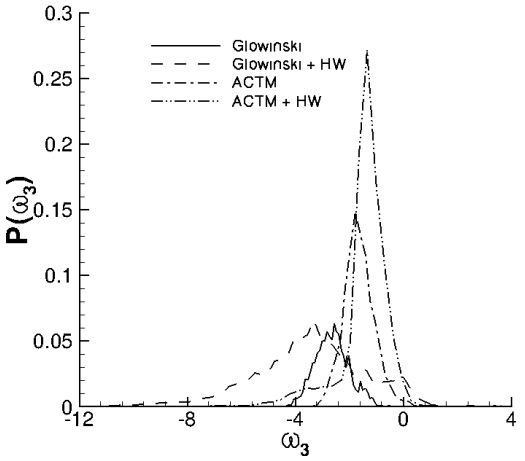

Figure 7. Probability density function of the angular velocity (rotation around spanwise axis) of the particle (creeping condition).

the path integral of the circumferential velocity should equal the path integral of the linear velocities. This was addressed by calculating a slipping length L_{slip} of the particle travelling in a creeping state defined as follows

$$L_{slip} = L_{circ} - L_{trans} \tag{8}$$

$$L_{circ} = \int_{t(x_{coll,i-1})}^{t(x_{coll,i})} |\omega(t) \times R|\, dt \tag{9}$$

$$L_{trans} = \int_{t(x_{coll,i-1})}^{t(x_{coll,i})} |\mathbf{u}_p(t)|\, dt \tag{10}$$

This is displayed in Fig. 8 for different values of L, i.e. the

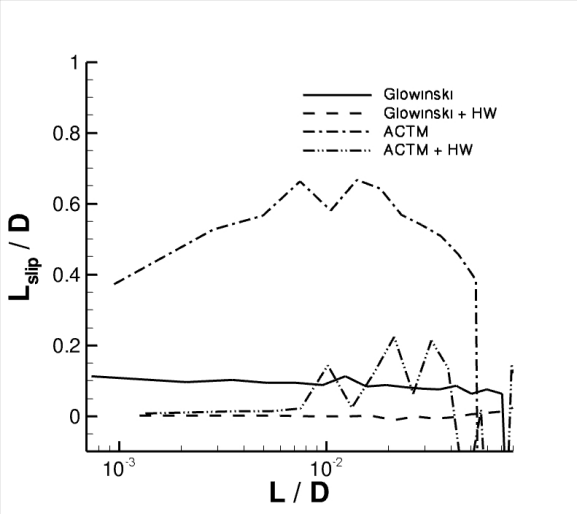

Figure 8. Slipping length of a moving particle in the creeping state.

distance between two collisions. For physically realistic models with tangential forces L_{slip} should be close to zero. Obviously, with decreasing L there is a considerable slip of the particle if a tangential model is absent, so that the particle stays in a constant rotational motion independent of the collision process.

To investigate the impact of the effects mentioned above, the overall percentage of time that a particle spends in one of the three kinematic states was calculated for the three different density ratios ρ_p/ρ_f employed (Fig. 9). With increasing particle density the impact of the collision model increases. Light particles spend most of the time in the jumping state far from the lower boundary with rare contact. Their trajectory hence is not as dependent on the collision model as for heavy particles. For the latter, the time spent in creeping state or resting state increases drastically. As discussed in the context of Fig. 6 the particle has a lower exposure with the ACTM because of the lower repulsive range S. Thus, the rebound height must be lower because of the lower hydrodynamic forces on the particle if the ACTM is used. The tangential model on the other hand leads to longer periods of creeping before the particle reaches a resting position again. While the particle stays in a constantly spinning motion without tangential contact, this is suppresed with a tangential model. With the hydrodynamic forces exceeding a given threshold, this angular momentum exerted on the particle by the fluid generates a rolling motion.

RESULTS FOR MANY MOBILE PARTICLES

With 500 mobile particles (Setup II), statistical data were collected for more than 30 flow through times (with the flow through time equal to the domain length divided by the bulk velocity of the fluid phase). The PDF of the wall normal position of the particles is shown in Fig. 10. Since the Froude number is relatively high with $Fr = 1.98$ the particles stay on average very close to the sediment bed. Only a few particles reach heights of more than one particle diameter. Due to the choice of the forcing range, $S = 2h$, the particle positions obtained with the RPM are generally higher than with

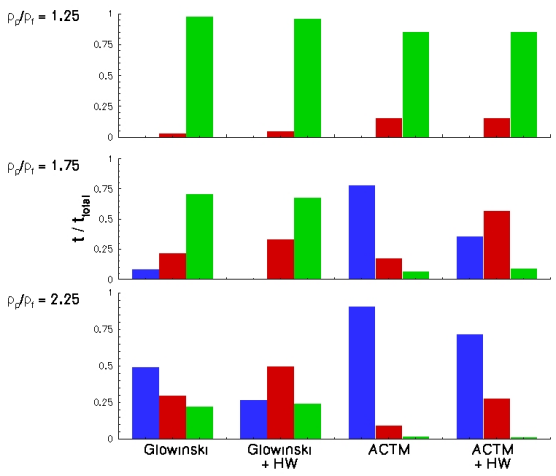

Figure 9. Overall time the particle spends in different kinematic states (1. bar: resting, 2. bar: creeping, 3. bar: jumping, from left to right).

the ACTM. On the other hand, including a tangential interaction model with ACTM or RPM does not substantially affect the wall normal distribution of the particles compared to simulations without tangential collision forces. The standard deviation of the wall normal position obtained in the simulations employing the RPM is generally larger than obtained in the simulations using the ACTM. This is an effect caused by the lubrication model for the under-resolved viscous forces (4) in the ACTM. Lubrication forces are dissipative and decelerate the particle for both, approach and rebound. Hence, the average jumping height is reduced with ACTM. The impact

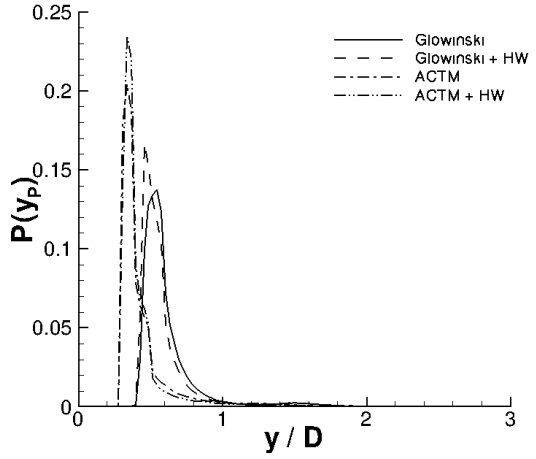

Figure 10. Probability density function of the wall normal position of the particle centers.

of the tangential force model can be appreciated in Fig. 11 showing the mean angular velocity of the particles in spanwise direction ω_3. Due to the very small number of samples for $y/D > 1.5$, the curves are not displayed in this region (cf. Fig. 10). It can be seen that the tangential force model yields a significant rotation of the particles with a strong peak of ω_3 in the first bin close to the bottom, demonstrating that indeed the particles roll over the bed. In the cases without tangential model, the rotation of the particles near the top of the bed is much smaller but not zero. The reason for this is generation of angular momentum by the strong velocity gradient in the fluid phase near the top of the bed. For comparison with

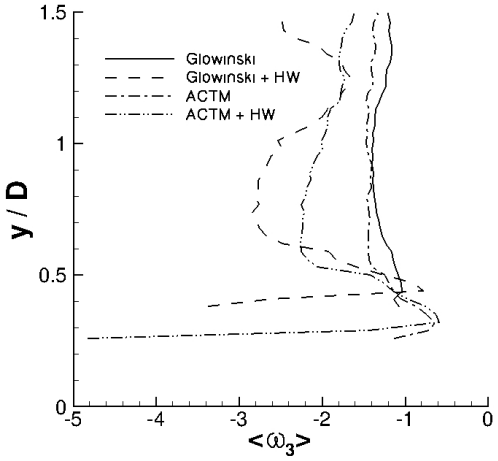

Figure 11. Mean angular velocity (rotation around spanwise axis) over height.

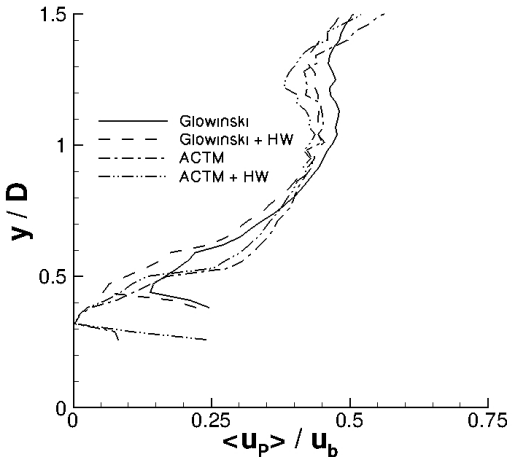

Figure 12. Mean particle velocity in streamwise direction over height.

experimental data, the well known Shields parameter S

$$S = \frac{u_\tau^2 \rho_f}{(\rho_p - \rho_f) g D_p} \tag{11}$$

can be compared to the critical Shields paramter S^* which indicates incipient sediment erosion (i.e. at least 10% of the sediment is in motion). While S is $2 \cdot 10^{-2}$ for the present configuration, the critical Shields number for incipient sediment motion gives $S^* = 3.5 \cdot 10^{-2}$ (Shields, 1936). Hence, no sediment transport should occur in the present case. Therefore a small volume-averaged particle velocity indicates physically plausible results.

The average streamwise velocity of the particles $\langle u_p \rangle$ (Fig. 12) in combination with the PDF of the wall normal position (Fig. 10) yields the volume averaged mean particle velocity (Tab. 2). It can be seen that the volume averaged-velocity of the particles is reduced when accounting for tangential forces and when employing ACTM instead of RPM. The ACTM with tangential force model yields the best results in comparison to the experimental data of Shields.

Table 2. Mean particle velocity normalized with the bulk velocity simulated by using different collision models.

Glowinski	Glowinski + HW	ACTM	ACTM + HW
0.247	0.181	0.121	0.093

CONCLUSIONS

In the sensitivity analysis presented in this paper for two different setups demonstrates that the choice of the collision model highly influences the modeling of sediment transport. Particles that show a high frequency of collision move faster and jump higher when the RPM is used. The key parameter that causes this difference is the repulsive range $S = 2h$ used in the Glowinski model. In addition, the use of a tangential model allows the particles to transform the hydrodynamic forces acting on the particle into a rolling motion if they are in contact with the sediment bed. For the simulation of incipient motion a proper choice of a collision model is one of the key factors to guarantee a high quality simulation. Comparison to experimental data indicates better results for collision models that take all the governing effects (both numerically and physically) into acount.

REFERENCES

Cameron, S. M., Coleman, S. E., Mellville, B. W. & I., Nikora V. 2006 Marbles in oil, just like a river? In *Proc. River Flow, Lisbon, Portugal, 927-935*.

Cox, R. G. & Brenner, H. 1967 Slow motion of a sphere through a viscous fluid towards a plane surface .2. small 99gap widths including inertial effects. *Chemical Engineering Science* **22** (12), 1753–&.

Glowinski, R., Pan, T. W., Hesla, T. I., Joseph, D. D. & Periaux, J. 2001 A fictitious domain approach to the direct numerical simulation of incompressible viscous flow past moving rigid bodies: Application to particulate flow. *Journal of Computational Physics* **169** (2), 363–426.

Haff, P. K. & Werner, B. T. 1986 Computer-simulation of the mechanical sorting of grains. *Powder Technology* **48** (3), 239–245.

Kempe, T, & Fröhlich, J. 2011 Collision modelling for the interface-resolved simulation of spherical particles in viscous fluids. *submitted* .

Kempe, T. & Fröhlich, J. 2010*a* Collision modeling for spherical particles in viscous fluids. In *7th International Conference on Multiphase Flow. Tampa, Florida, USA*.

Kempe, T. & Fröhlich, J. 2010*b* On Euler-Lagrange coupling and collision modelling for spherical particles. In *8th International ERCOFTAC Symposium on Engineering Turbulence Modelling and Measurements, Marseille, France*.

Kempe, T., Schwarz, S. & Fröhlich, J. 2009 Modelling of spheroidal particles in viscous flow. In *Academy Colloquium Immersed Boundary Methods: Current Status and Future Research Directions, Amsterdam, the Netherlands*.

Lajeunesse, E., Malverti, L. & Charru, F. 2010 Bed load transport in turbulent flow at the grain scale: Experiments and modeling. *Journal of Geophysical Research-earth Surface* **115**, F04001.

Shields, A. 1936 Anwendung der Aehnlichkeitsmechanik und der Turbulenzforschung auf die Gewschiebebewegung. PhD thesis, Mitteilungen der Preußischen Versuchsanstalt für Wasserbau und Schiffbau, Berlin.

Uhlmann, M. 2005 An immersed boundary method with direct forcing for the simulation of particulate flows. *Journal of Computational Physics* **209** (2), 448–476.